doi: 10.12029/gc2020Z104

论文引用格式：王文龙, 刘洋, 赵利刚, 滕飞, 杨泽黎. 2020. 华北板块北缘中段二叠纪岩浆岩年代学、地球化学及锆石 Hf 同位素测试数据集 [J].中国地质，47(S1):32−39.

数据集引用格式：王文龙; 刘洋; 赵利刚; 滕飞; 杨泽黎. 华北板块北缘中段二叠纪岩浆岩年代学、地球化学及锆石 Hf 同位素测试数据集 (V1). 中国地质调查局天津地质调查中心 [创建机构], 2016. 全国地质资料馆 [传播机构], 2020-06-30. 10.35080/data.A.2020.P4; http://dcc.cgs.gov.cn/cn//geologicalData/details/doi/10.35080/data.A.2020.P4

收稿日期：2020-04-04
改回日期：2020-04-24

基金项目：本文由中国地质调查局地质调查项目（DD20160041、DD20190038）资助。

华北板块北缘中段二叠纪岩浆岩年代学、地球化学及锆石 Hf 同位素测试数据集

王文龙　刘洋*　赵利刚　滕飞　杨泽黎

(中国地质调查局天津地质调查中心，天津 300170)

摘要：华北板块北缘中段位于华北板块与白乃庙弧的结合处，以赤峰-白云鄂博断裂为界，南、北归属不同的大地构造单元，并且具有不同的基底属性。二叠纪岩浆岩在华北板块北缘广泛分布，断裂带两侧均有出露，源区组成十分复杂，制约着对其岩石成因及构造背景的深刻认识。本文通过对横跨赤峰–白云鄂博断裂的“北柳图庙幅等 4 幅区调”和“乌兰布拉格幅等 2 幅区调”2 个项目的 1∶50 000 区调工作，共计 6 个 1∶50 000 图幅内的二叠纪岩浆岩的年代学、地球化学及锆石 Hf 同位素测试数据进行整合、分析，为进一步研究华北板块北缘中段二叠纪岩浆岩的源区及构造-岩浆演化过程提供详实的数据支撑。区内二叠纪侵入岩广泛出露，岩石类型以花岗闪长岩、(石英）闪长岩及二长花岗岩为主，并含有少量的正长花岗岩。二叠纪火山岩主要分布在断裂带以南，岩性包括安山质、英安质及少量流纹质火山岩。锆石 U–Pb 测年表明工作区内二叠纪岩浆岩的形成时代主要为中–晚二叠世，断裂带南北两侧的岩浆岩具有截然不同的锆石 Hf 同位素特征，总体而言，南侧相对富集，北侧相对亏损。本数据集包括 3 个.xls 类型文件（Zircon U–Pb dating data.xls，Zircon Hf isotope data.xls，Whole-rock geochemistry data.xls），分别记录了 104 件样品的地球化学数据、16 件样品的锆石 U–Pb 测年数据和 12 件样品的锆石 Hf 同位素数据。本数据集测试样品主要在中国地质调查局天津地质调查中心实验测试中心完成，数据质量可靠。

关键词：锆石U–Pb测年；锆石Hf同位素；岩石地球化学；二叠纪岩浆岩；白乃庙弧；华北板块北缘

数据服务系统网址：http://dcc.cgs.gov.cn

1　引言

中亚造山带夹持于西伯利亚、塔里木、华北和欧洲板块之间（图 1a；Jahn BM et al., 2000; Windley BF et al., 2007; Han BF et al., 2011; Xiao WJ et al., 2015; Zhou H et al.,

第一作者简介：王文龙，男，1988 年生，硕士研究生，构造地质学专业；E–mail：wenlon0417@163.com。
通讯作者简介：刘洋，男，1986 年生，硕士研究生，构造地质学专业；E–mail：125313766@qq.com。

2018），是显生宙陆壳增生与改造最显著的造山带之一（Şengör AMC et al., 1993; Windley BF et al., 2007）。中亚造山带的演化经历了古亚洲洋的俯冲、岛弧迁移及地块增生等一系列地质事件。华北板块北缘古生代构造-岩浆活动强烈，对于研究中亚造山带古生代的构造演化历史具有重要意义（Xiao WJ et al., 2003, 2015）。

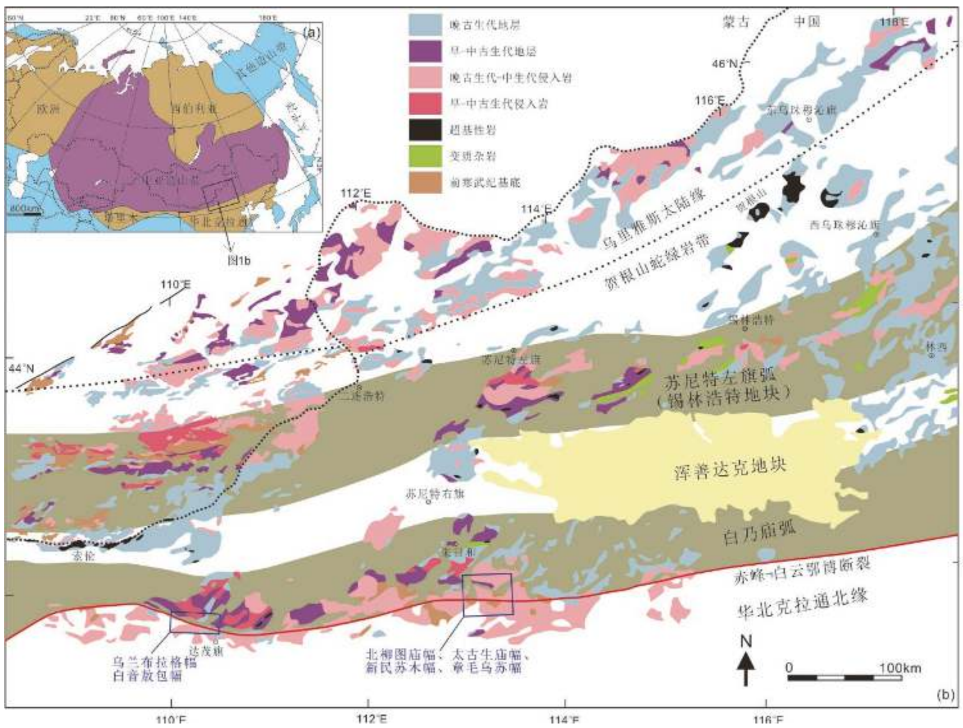

图 1　中亚造山带构造纲要图（a，据 Han BF et al., 2011 修改；）和
中亚造山带东南段构造纲要图（b，据 Chen Y et al., 2020 修改）

华北板块北缘与白乃庙弧相连，二者以近东西向延伸的赤峰–白云鄂博断裂为界（图 1b； 内蒙古自治区地质矿产局, 1991）。目前的研究普遍认为：早古生代时期，古亚洲洋内存在洋内俯冲，形成了白乃庙弧，而在早古生代末期，白乃庙弧与华北板块北缘发生拼合（Chen Y et al., 2020; Zhou H et al., 2018; Zhang SH et al., 2014），至晚古生代时期，古亚洲洋板块持续向南俯冲，致使华北板块北缘逐渐转化为成熟的大陆弧（Zhang SH et al., 2009, 2016; Zhou H et al., 2019）。研究区内古生代构造-岩浆活动强烈，其中早古生代岩浆岩集中分布于赤峰–白云鄂博断裂以北的白乃庙弧，晚古生代岩浆岩在断裂两侧均有出露（图 1b），以二叠纪岩浆活动最为强烈，岩石类型十分丰富（罗红玲等, 2009； Zhang SH et al., 2009, 2016, 2017；王挽琼等, 2013；董晓杰等, 2016; Zhao P et al., 2013; Zhou H et al., 2019）。对于二叠纪岩浆岩的成因及构造环境目前存在较大的争议，主要存在 2 种观点：一种观点认为二叠纪华北板块北缘处于后碰撞伸展环境，形成 A 型花岗岩及双峰式岩浆岩（罗红玲等, 2009；Zhao P et al., 2013），同时期形成的具有弧性质的岩浆岩可能继承了早期岛弧岩浆岩的地球化学特征（Zhao P et al., 2013）；另一种观点则认为二叠纪华北板块北缘处于活动大陆边缘环境，形成一系列弧型花岗岩（Zhang SH et al., 2009, 2016, 2017; 王挽琼等, 2013； 董晓杰等, 2016；王师捷等, 2018；朱雪峰等, 2018；Zhou H et al., 2019），而 A 型花岗岩形成于随后的后碰撞环境（罗红玲等, 2009； Zhou H et al., 2019）。

岩浆岩的形成受源区物质组分、部分熔融程度、物理化学条件及岩浆冷却过程多种因素控制，因而不同成因的岩浆岩往往具有不同的地球化学特征（罗照华等, 2007；王孝磊等, 2017），而在各种影响因素中，源区物质组分在控制岩石地球化学成分上起着主导作用（Clemens JD et al., 2011; Champion DC and Bultitude RJ, 2013）。华北板块与白乃庙岛弧具有不同的基底属性（Zhang SH et al., 2014），所形成的晚古生代岩浆岩具有复杂的源区组成及截然不同的锆石 Hf 同位素特征（图 2； Zhang SH et al., 2009, 2016, 2017; 董晓杰等, 2016; 朱雪峰等, 2018; Zhou H et al., 2019），因此明确华北板块北缘与白乃庙弧内晚古生代岩浆岩各自的源区性质是探讨岩石成因及构造–岩浆演化过程的基础。

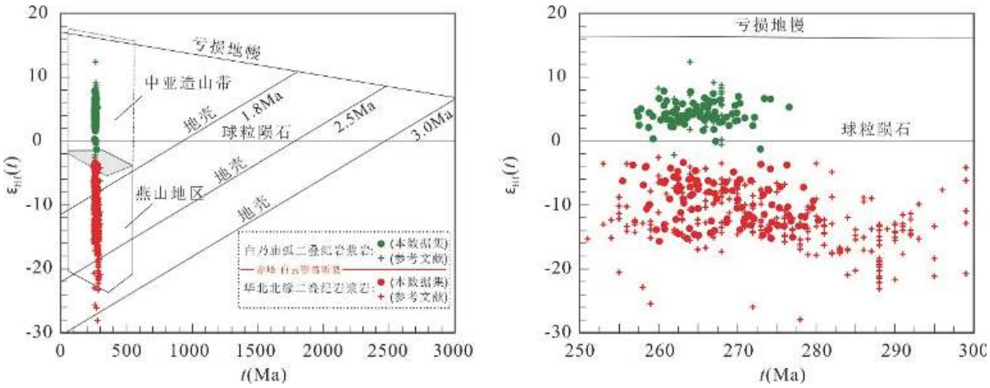

图 2　华北北缘中段二叠纪岩浆岩 ε_{Hf}（t）–t 图解（参考文献数据点引自 Zhang SH et al., 2009, 2016； 董晓杰等, 2016； 朱雪峰等, 2018；Zhou H et al., 2019**）**

内蒙古 1：50 000 北柳图庙幅（K49E011021）、太古生庙幅（K49E011022）、新民苏木幅（K49E01 2021）、章毛乌苏幅（K49E01 2022）区域地质矿产调查（以下简称“北柳图庙幅等 4 幅区调项目”）及内蒙古 1: 50 000 乌兰布拉格幅（K49E013008）、白音敖包幅（K49E013009）幅区域地质调查（以下简称“乌兰布拉格幅等 2 幅区调项目”）的图幅范围位于华北北缘与白乃庙弧的结合位置。赤峰–白云鄂博断裂从研究区中部通过。区内广泛出露二叠纪岩浆岩，对于断裂南、北两侧二叠纪岩浆岩年代学、地球化学及锆石 Hf 同位素数据集的建立可以为研究区域二叠纪岩浆岩的源区组成及构造-岩浆演化过程提供重要的数据支撑。

华北板块北缘中段二叠纪岩浆岩年代学、地球化学及锆石 Hf 同位素测试数据集（王文龙等, 2020）元数据简介见表 1。

2　数据采集和处理方法

2.1　样品采集

本次采集的二叠纪岩浆岩样品位于朱日和南的北柳图庙幅等 4 幅区调项目（工作区范围：东经 113°00' ~ 113°30'，北纬 42°00' ~ 42°20'）以及位于达茂旗北西的乌兰布拉格幅等 2 幅区调项目（工作区范围：东经 109°45' ~ 110°15'，北纬 41°50' ~ 42°00'）调查区。北柳图庙幅等 4 幅区调项目对二叠纪侵入岩进行了锆石 U–Pb 测年、锆石 Hf 同位素及全岩地球化学分析，岩石样品取自石英闪长岩、花岗闪长岩及二长花岗岩。其中，锆石 U–Pb 测年样品 10 件，锆石 Hf 同位素 9 件，全岩地球化学分析 77 件。乌兰布拉格幅等 2 幅

表 1　数据库（集）元数据简表

条目	描述
数据库（集）名称	华北板块北缘中段二叠纪岩浆岩年代学、地球化学及锆石Hf同位素测试数据集
数据库（集）作者	王文龙，中国地质调查局天津地质调查中心 刘　洋，中国地质调查局天津地质调查中心 赵利刚，中国地质调查局天津地质调查中心 滕　飞，中国地质调查局天津地质调查中心 杨泽黎，中国地质调查局天津地质调查中心
数据时间范围	2016–2019年
地理区域	北柳图庙幅等4幅区调地理坐标范围：东经 113°00'～113°30'，北纬42°00'～42°20' 乌兰布拉格幅等2幅区调地理坐标范围：东经 109°45'～110°15'，北纬41°50'～42°00'
数据格式	*.xls
数据量	948 kB
数据服务系统网址	http://dcc.cgs.gov.cn
基金项目	中国地质调查局地质调查项目（DD20160041、DD20190038）
语种	中文
数据库（集）组成	数据集由3个Excel数据组成，分别为“Zircon U–Pb dating data.xls”、“Zircon Hf isotope data.xls”和“Whole-rock geochemistry data.xls”，每个Excel数据又进一步分为“北柳图庙幅等4幅区调项目数据”及“乌兰布拉格幅等2幅区调项目数据”两个独立工作表。其中，“Zircon U–Pb dating data.xls”为锆石测年数据，包括16件测年样品（测点总数401个）；“Whole-rock geochemistry data.xls”为全岩地球化学数据，包括104件测试样品。“Zircon Hf isotope data.xls”为锆石Hf同位素数据，包括12件样品（测点总数191个）

区调项目对二叠纪侵入岩及火山岩进行了锆石 U–Pb 测年、锆石 Hf 同位素及全岩地球化学分析，侵入岩岩石类型主要为花岗闪长岩及二长花岗岩，火山岩主要为安山质、英安质及流纹质火山碎屑岩，少量为火山熔岩。其中，锆石 U–Pb 测年样品 6 件，锆石 Hf 同位素 3 件，全岩地球化学分析 27 件。样品编号、岩石类型及采样位置详见数据集。

2.2　测试方法

2.2.1　锆石 U-Pb 测年及 Hf 同位素分析

野外采集新鲜的锆石测年样品，锆石分选在河北省区域地质调查研究所实验室进行，在对样品进行水粗淘、强磁分选、电磁分选和酒精细淘之后，在显微镜下挑选出颗粒大、形态完整的锆石。锆石制靶在北京锆年领航科技有限公司完成，并使用日本电子 JSM_6510 型扫描电镜完成锆石阴极发光照相。锆石 U–Pb 年龄测试及原位 Hf 同位素测试在天津地质调查中心实验室利用激光剥蚀多接收器电感耦合等离子体质谱仪（LA–MC–ICPMS）完成，将 NEW WAVE 193–FXArF 准分子激光器与 Thermo Fisher 公司的 Neptune 多接收器电感耦合等离子体质谱仪联接，采用 He 气作为剥蚀物质的载气，锆石 U–Pb 年龄测定采用的激光束斑直径为 35 μm，剥蚀时间为 30 s，采用 GJ–1 作为校正标样校正锆石的 U、Th 和 Pb 同位素分馏；采用 NIST610 玻璃作为外标计算锆石中 U、Th 和 Pb 含量。测试过程中每隔 8 个样品测试点，进行两个 GJ–1 标样点测试，

GJ–1 的^{206}Pb/^{238}U 加权平均年龄为 600 Ma。

锆石原位微区 Hf 同位素分析采用与 U-Pb 年龄测定相同的激光器与质谱仪，激光剥蚀束斑直径为 50 μm，剥蚀时间为 30 s，采用 GJ–1 作为外标计算 Hf 同位素比值，测试过程中每隔 8 个样品测试点，进行两个 GJ–1 标样点测试，GJ–1 的^{176}Hf/^{177}Hf 和^{176}Lu/^{177}Hf 测定结果分别为 0.282019±0.000024（2σ，n=57）和 0.00030（n=57）。具体仪器配置和实验流程参见李怀坤等 (2010) 和耿建珍等 (2011)。U–Pb 测年和 Hf 同位素数据处理采用 ICPMSDataCal 程序（Liu YS et al., 2010）。

2.2.2　全岩地球化学

野外采集新鲜的岩石样品，首先用水将样品表面冲洗干净并晾干，机械破碎至 200 目后送实验室分析。岩石主量和微量元素分析在天津地质调查中心实验室完成，主量元素用熔片法 X 射线荧光光谱法 (XRF) 测试，FeO 采用氢氟酸、硫酸溶样、重铬酸钾滴定容量法，分析精度优于 2%，微量元素使用 ICP–MS 测试，分析精度优于 5%。测试过程中采用 GBW07104、GBW07105、GBW07111、GBW07122 做为标样。检测依据 GB/T 14506–2010，检测环境为温度 20℃，湿度 30%。

3　数据样本描述

华北北缘中段二叠纪岩浆岩年代学、地球化学及锆石 Hf 同位素测试数据集为 Excel 表格型数据，包括 3 个 Excel 数据文件，分别为“Zircon U–Pb dating data.xls”、“Zircon Hf isotope data.xls”及“Whole-rock geochemistry data.xls”，每个 Excel 数据又进一步分为“北柳图庙幅等 4 幅区调项目数据”及“乌兰布拉格幅等 2 幅区调项目数据”2 个独立工作表。

“Zircon U-Pb dating data.xls”数据文件为研究区内 16 件样品的锆石 U-Pb 年龄信息，每个工作表中包含样品编号、采样点、岩石类型、分析点号、Th/U、同位素比值、年龄、误差等数据。“Zircon Hf isotope data.xls”数据文件为研究区内 12 件样品锆石 Hf 同位素测试数据，每个工作表中包含样品编号、分析点号、锆石年龄、同位素比值，$\varepsilon_{Hf}(t)$ 及模式年龄等数据。“Whole-rock geochemistry data.xls”数据文件为研究区内 104 件样品的主量和微量元素分析结果，每个工作表中包含样品编号、岩石类型与全岩地球化学分析结果，详见数据集。

4　数据质量控制与评估

锆石 U–Pb 年龄、Hf 同位素组成及全岩地球化学分析均在中国地质调查局天津地质调查中心实验室完成。测试方法与过程均严格遵守国际标准进行（任军平等, 2019；王树庆等, 2019）。用于测试的二叠纪岩浆岩并没有经历明显的变质和交代作用，岩石样品总体较为新鲜。测年样品中锆石晶形完整、环带发育，但部分锆石受后期构造应力的影响存在裂隙，测试点位需要避开锆石裂隙（李崇等, 2018)。LA–ICP–MS 锆石 U–Pb 测年实验的过程与侯可军等 (2009) 所采用方法基本一致，锆石 Hf 同位素分析过程与侯可军等 (2007) 方法基本一致，所测得的锆石年龄结果及 Hf 同位素分析结果可以与区域上其他学者数据结果进行对比（王挽琼等, 2013；董晓杰等, 2016；朱雪峰等, 2018；Zhou H et al., 2019）。

5 结论

华北板块北缘中段二叠纪岩浆岩年代学、地球化学及锆石 Hf 同位素测试数据集由 3 个 Excel 数据组成，分别为“Zircon U–Pb dating data.xls”、“Zircon Hf isotope data.xls”及“Whole-rock geochemistry data.xls”。其中，“Zircon U–Pb dating data.xls”为锆石测年数据，包括 16 件测年样品；“Whole-rock geochemistry data.xls”为全岩地球化学数据，包括 104 件测试样品。“Zircon Hf isotope data.xls”为锆石 Hf 同位素数据，包括 12 件样品。该数据集可以为研究区域二叠纪岩浆岩的源区组成及构造–岩浆演化过程提供关键的基础性数据。

致谢：两位匿名审稿人对论文提出了宝贵修改意见，在此致以诚挚的谢意！

参考文献

Champion DC, Bultitude RJ. 2013. The geochemical ang Sr-Nd isotopic characteristics of Paleozoic fractionated S-types granites of north Queensland: Implications for S-type granite petrogenesis[J]. Lithos, 162–163: 37−56.

Chen Y, Zhang ZC, Qian XQ, Li JF, Ji ZJ, Wu TR. 2020. Early to mid-Paleozoic magmatic and sedimentary records in the Bainaimiao Arc: An advancing subduction-induced terrane accretion along the northern margin of the North China Craton[J]. Gondwana Research, 79: 263−282.

Clemens JD, Stevens G, Farina F. 2011. The enigmatic sources of I-type granites: The peritectic connexion[J]. Lithos, 126: 174−181.

Han BF, He GQ, Wang XC, Guo ZJ. 2011. Late Carboniferous collision between the Tarim and Kazakhstan eYili terranes in the western segment of the South Tian Shan Orogen, Central Asia, and implications for the Northern Xinjiang, western China[J]. Earth-Science Reviews, 109: 74−93.

Jahn BM, Wu FY, Chen B. 2000. Massive granitoid generation in Central Asia: Nd isotope evidence and implication for continental growth in the Phanerozoic[J]. Episodes, 23: 82−92.

Liu YS, Gao S, Hu ZC, Gao CG, Zong KQ, Wang DB. 2010. Continental and oceanic crust recycling-induced melt-peridotite interactions in the Trans-North China Orogen: U-Pb dating, Hf isotopes and trace elements in zircons from mantle xenoliths[J]. Journal of Petrology, 51: 537−571.

Sengör AMC, Natal'in BA, Burtman VS. 1993. Evolution of Altaid tectonic collageand Paleozoic crustal growth in Eurasia[J]. Nature, 364: 299−307.

Windley BF, Alexeiev D, Xiao W, Kröner A, Badarch G. 2007. Tectonic models for accretion of the Central Asian Orogenic Belt[J]. Journal of the Geological Society of London, 164: 31−47.

Xiao WJ, Windley BF, Hao J, Zhai MG. 2003. Accretion leading to collision and the Permian Solonker suture, Inner Mongolia, China: termination of the central Asian orogenic belt[J]. Tectonics, 22: 1069.

Xiao WJ, Windley BF, Sun S, Li J, Huang B, Han C, Yuan C, Sun M, Chen H. 2015. A tale of amalgamation of three permo-triassic collage systems in central Asia: oroclines, sutures, and terminal accretion[J]. Annual Review of Earth and Planetary Sciences, 43: 477−507.

Zhang SH, Zhao Y. 2017. Cogenetic origin of mafic microgranular enclaves in calc-alkaline granitoids: The Permian plutons in the northern North China Block[J]. Geosphere, 13: 482−517.

Zhang SH, Zhao Y, Ye H, Liu JM, Hu CZ. 2014. Origin and evolution of the Bainaimiao arc belt:

implications for crustal growth in the southern Central Asian Orogenic Belt[J]. Geological Society of America Bulletin, 126: 1275−1300.

Zhang SH, Zhao Y, Ye H, Liu JM, Hu ZC. 2016. Different sources involved in generation of continental arc volcanism: The Carboniferous-Permian volcanic rocks in the northern margin of the North China block[J]. Lithos, 240–243: 382−401.

Zhang SH, Zhao Y, Kröner A, Liu XM, Lie WX, Chen FK. 2009. Early Permian Plutons from the Northern North China Block:Constraints on Continental Arc Evolution and Convergent Margin Magmatism Relatedtothe Central Asian Orogenic Belt[J]. International Journal of Earth Sciences, 98(6): 1441−1467.

Zhao P, Chen Y, Xu B, Faure M, Shi, G, Choulet F. 2013. Did the Paleo-Asian Ocean between North China Block and Mongolia Block exist during the late Paleozoic? First paleomagnetic evidence from central-eastern Inner Mongolia, China[J]. Journal of Geophysical Research, Solid Earth, 118: 1873−1894.

Zhou H, Zhao GC, Han YG, Wang B. 2018. Geochemistry and zircon U-Pb-Hf isotopes of Paleozoic intrusive rocks in the Damao area in Inner Mongolia, northern China: Implications for the tectonic evolution of the Bainaimiao arc[J]. Lithos, 314–315: 119−139.

Zhou H, Zhao GC, Li JH, Han YG, Yao JL, Wang B. 2019. Magmatic evidence for middle-late Permian tectonic evolution on the northern margin of the North China Craton[J]. Lithos, 336–337: 125−142.

Zhou JB, Wilde SA, Zhao GC, Han J. 2018. Nature and assembly of microcontinental blocks within the Paleo-Asian Ocean[J]. Earth-Science Reviews, 186: 76−93.

董晓杰, 王挽琼, 沙茜, 张金凤. 2016. 华北克拉通北缘中段二叠纪苏吉火山岩及其形成机制 [J]. 岩石学报, 32(9): 2765−2779.

耿建珍, 李怀坤, 张健, 周红英, 李惠民. 2011. 锆石 Hf 同位素组成的 LA-MC-ICP-MS 测定 [J]. 地质通报, 30(10): 1508−1513.

侯可军, 李延河, 田有荣. 2009. LA-MC-ICP-MS 锆石微区原位 U-Pb 定年技术 [J]. 矿床地质, 28(4): 481−492.

侯可军, 李延河, 邹天人, 曲晓明, 石玉若, 谢桂青. 2007. LA-MC-ICP-MS 锆石 Hf 同位素的分析方法及地质应用 [J]. 岩石学报, 23(10): 2595−2604.

李崇, 任留东. 2018. 辽北清原杂岩锆石年代学与地球化学测试数据集 [J]. 中国地质, 45(S1): 94−101.

李怀坤, 朱士兴, 相振群, 苏文博, 陆松年, 周红英, 耿建珍, 李生, 杨锋杰. 2010. 北京延庆高于庄组凝灰岩的锆石 U-Pb 定年研究及其对华北北部中元古界划分新方案的进一步约束 [J]. 岩石学报, 26(7): 2131−2140.

罗红玲, 吴泰然, 赵磊. 2009. 华北板块北缘乌梁斯太 A 型花岗岩体锆石 SHRIMP U-Pb 定年及构造意义 [J]. 岩石学报, 25(3): 515−526.

罗照华, 黄忠敏, 柯珊. 2007. 花岗质岩石的基本问题 [J]. 地质论评, 53(S1): 180−226.

内蒙古自治区地质矿产局. 1991. 内蒙古自治区区域地质志 [M]. 北京: 地质出版社.

任军平, 王杰, 古阿雷, 左立波, 孙宏伟, 许康康, 吴兴源. 2019. 赞比亚东北部正长花岗岩的锆石 U-Pb 年龄和 Lu-Hf 同位素特征 [J]. 地质调查与研究, 42(3): 161−165.

王师捷, 徐仲元, 董晓杰, 王挽琼, 李鹏川. 2018. 华北板块北缘中段花岗闪长岩-苏长辉长岩的锆石

U-Pb 年代学、地球化学特征及其形成机制 [J]. 地球科学, 43(9): 3267−3284.

王树庆, 胡晓佳, 赵华雷. 2019. 内蒙古苏左旗洪格尔地区新发现晚石炭世碱性花岗岩 [J]. 地质调查与研究, 42(2): 81−85.

王挽琼, 徐仲元, 刘正宏, 赵庆英, 蒋孝君. 2013. 华北板块北缘中段早中二叠世的构造属性:来自花岗类锆石 U-Pb 年代学及地球化学的制约 [J]. 岩石学报, 29(9): 2987−3003.

王文龙, 刘洋, 赵利刚, 滕飞, 杨泽黎. 2020. 华北板块北缘中段二叠纪岩浆岩年代学、地球化学及锆石 Hf 同位素测试数据集 [DB/OL]. 地质科学数据出版系统. (2020-06-30). DOI:10.35080/data.A.2020.P4.

王孝磊. 2017. 花岗岩研究的若干新进展与主要科学问题 [J]. 岩石学报, 33(5): 1445−1458.

朱雪峰, 陈衍景, 王玭, 张成, 蔡云龙, 邓柯, 许强伟, 李凯月. 2018. 内蒙古毕力赫斑岩型金矿成矿岩体地球化学、锆石 U-Pb 年代学及 Hf 同位素研究 [J]. 地学前缘, 25(5): 120−134.

doi: 10.12029/gc2020Z104

Article Citation: Wang Wenlong, Liu Yang, Zhao Ligang, Teng Fei, Yang Zeli. 2020. Dataset of Chronology, Geochemistry and Zircon Hf Isotopes of Permian Magmatites in the Middle Section of the Northern Margin of North China Craton[J]. Geology in China, 47(S1):44−53.

Dataset Citation: Wang Wenlong; Liu Yang; Zhao Ligang; Teng Fei; Yang Zeli. Dataset of Chronology, Geochemistry and Zircon Hf Isotopes of Permian Magmatites in the Middle Section of the Northern Margin of North China Craton(V1). Tianjin Center, China Geological Survey[producer], 2016. National Geological Archives of China [distributor], 2020-06-30. 10.35080/data.A.2020.P4; http://dcc.cgs.gov.cn/en//geologicalData/details/doi/10.35080/data.A.2020.P4.

Received: 04-04-2020
Accepted: 24-04-2020

Fund Project:
The geological survey projects (DD20160041, DD20190038) initiated by China Geological Survey

Dataset of Chronology, Geochemistry and Zircon Hf Isotopes of Permian Magmatites in the Middle Section of the Northern Margin of North China Craton

WANG Wenlong, LIU Yang*, ZHAO Ligang, TENG Fei, YANG Zeli

(*Tianjin Center*, *China Geological Survey*, *Tianjin* 300170, *China*)

Abstract: The middle section of the northern margin of the North China Craton (also referred to as the study area) is situated in the junction between the North China Craton and Bainaimiao arc. With the Chifeng–Bayan Obo fault as the boundary, its southern and northern parts fall within different geotectonic units and have different basement features. Permian magmatites are widely distributed across the northern margin of the North China Craton and are exposed on both sides of the fault zone. Their provenance consists of very complex components, constricting fuller understanding of the petrogenesis and tectonic background of the magmatites. The Chifeng–Bayan Obo fault is covered by two geological survey projects, one involves four map sheets including the Beiliutumiao map sheet, and the other covers two map sheets including the Wulanbulage map sheet. In this paper, the testing data of chronology, geochemistry, and zircon Hf isotopes of the Permian magmatites in all six map sheets from the two projects were integrated and analyzed based on the regional geological surveys on a scale of 1∶50 000 of the two projects. The aim is to provide detailed and accurate data for further research of the provenance and the tectonic-magmatic evolution process of Permian magmatites in the study area. Furthermore, Permian intrusions are also widely exposed in the study area, which mainly include granodiorites, (quartz) diorite, monzogranite, and a small number of syenite granites. Permian volcanics are mainly distributed to the south of the fault zone and consist of andesitic and dacitic volcanics as well as a small number of rhyolitic volcanics. As shown by zircon U–Pb dating, the Permian magmatites within the study area were mainly formed in mid–late Permian, and the magmatites on the northern and southern sides of the fault zone have distinctly different zircon Hf isotopic characteristics. In short, zircon Hf isotopes are rich on the southern side but depleted on the northern side. The datasets

About the first author: WANG Wenlong, male, born in 1988, master degree, majored in structural geology; E-mail: wenlon0417@163.com.

The corresponding author: LIU Yang, male, born in 1986, master degree, majored in structural geology; E-mail: 125313766@qq.com.

of chronology, geochemistry and zircon Hf isotopes of Permian magmatites in the study area (also referred to as the Dataset) include three.xls files (*Zircon U–Pb dating data.xls*, *Zircon Hf isotope data.xls* and *Whole-rock geochemistry data.xls*), which are comprised of data on the petrogeochemistry of 104 samples, zircon U–Pb dating of 16 samples and zircon Hf isotopes of 12 samples. Samples collected for the Dataset were mainly tested in the Experiment and Test Center of Tianjin Center, China Geological Survey, and thus the data obtained are credible.

Key words: zircon U–Pb dating; zircon Hf isotope; petrogeochemistry; Permian magmatite; Bainaimiao arc; Northern margin of North China Craton

Data service system URL: http://dcc.cgs.gov.cn

1 Introduction

The Central Asian Orogenic Belt is surrounded closely by the plates of Siberia, Tarim, North China and Europe (Fig. 1a; Jahn BM et al., 2000; Windley BF et al., 2007; Han BF et al., 2011; Xiao WJ et al., 2015; Zhou H et al., 2018). It is one of the orogens with the most significant accretion and transformation of Phanerozoic continental crust (Şengör AMC et al., 1993; Windley BF et al., 2007) and experienced a range of geological events such as subduction, island-arc migration and block accretion caused by the Paleo-Asian Ocean. The northern margin of the North China Craton went through intense Paleozoic tectonic-magmatic activities, and thus is very important to the research of the Paleozoic tectonic evolution history of the Central Asian Orogenic Belt (Xiao WJ et al., 2003, 2015).

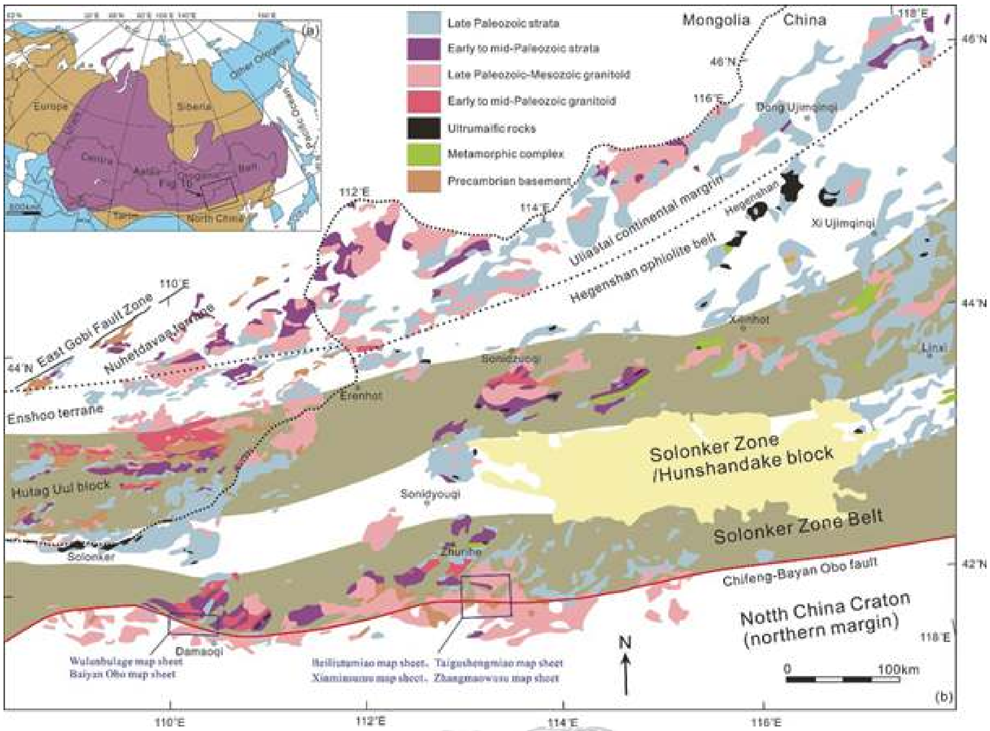

Fig. 1 Generalized geological maps of the Central Asian Orogenic Belt (a, modified after Han BF et al., 2011) and the southeastern part of the Central Asian Orogenic Belt (b, modified after Chen Y et al., 2020)

The northern margin of the North China Craton is connected with the Bainaimiao arc, with the Chifeng–Bayan Obo fault almost acting as a boundary extending in an east-west trending (Fig. 1b; Inner Mongolia Bureau of Geology and Mineral Resources Exploration and Development, 1991). The following views are generally shared by recent research. In the early Paleozoic, intra-oceanic subduction occurred in the Paleo-Asian Ocean, resulting in the formation of the Bainaimiao arc. At the end of the early Paleozoic, the Bainaimiao arc merged with the northern margin of the North China Craton (Chen Y et al., 2020; Zhou H et al., 2018; Zhang SH et al., 2014). By the late Paleozoic, the northern margin of the North China Craton was gradually transformed into a mature continental arc owing to continuous subduction of the Paleo-Asian Ocean Plate towards the south (Zhang SH et al., 2009, 2016; Zhou H et al., 2019). The study area went through intense Paleozoic tectonic-magmatic activities. The early Paleozoic magmatites are mainly distributed within the Bainaimiao arc that lies to the north of the Chifeng–Bayan Obo fault, with the late Paleozoic magmatites being exposed on both sides of the fault (Fig. 1b). The Permian magmatic activities feature the highest intensity in this area and thus a wide variety of Permian magmatites were formed (Luo HL et al., 2009; Zhang SH et al., 2009, 2016, 2017; Wang WQ et al., 2013; Dong XJ et al., 2016; Zhao P et al., 2013; Zhou H et al., 2019). The petrogenesis and tectonic environment of Permian magmatites are currently under dispute and are mainly backed by two opinions. One is that the northern margin of the North China Craton was in a tectonic environment of post-collision extension in the Permian and, as a result, A-type granites and bimodal magmatites were formed (Luo HL et al., 2009; Zhao P et al., 2016); meanwhile, the contemporaneous magmatites with arcuate occurrence possibly could have inherited the geochemical characteristics of the early island-arc magmatites (Zhao P et al., 2013). The other is that the northern margin of the North China Craton was in a tectonic environment of active continental margin in the Permian, leading to the formation of a series of arc-like granites (Zhang SH et al., 2009, 2016, 2017; Wang WQ et al., 2013; Dong XJ et al., 2016; Wang SJ et al., 2018; Zhu XF, 2018; Zhou H et al., 2019), and so, A-type granites were formed in the subsequent post-collision settings (Luo HL et al., 2009; Zhou H et al., 2019).

The formation of magmatites depends on multiple factors, such as material composition of provenance, degree of partial melting, physical and chemical conditions and the cooling process of magma. Therefore, magmatites with different geneses tend to have different geochemical characteristics (Luo ZH et al., 2007; Wang XL et al., 2017). However, the material composition of the provenance among the aforementioned factors plays a leading role in controlling the geochemical components within the rocks (Clemens JD et al., 2011; Champion DC and Bultitude RJ, 2013). North China Craton has different basement features from the Bainaimiao arc (Zhang et al., 2014). As a result, the late Paleozoic magmatites formed in these two places have a complex material composition of the provenance and distinctly different zircon Hf isotopic characteristics (Fig. 2; Zhang SH et al., 2009, 2016, 2017; Dong XJ et al., 2016; Zhu XF et al., 2018; Zhou H et al., 2019). Therefore, ascertaining the respective provenance features of the late Paleozoic magmatites in the two places will lay a basis for

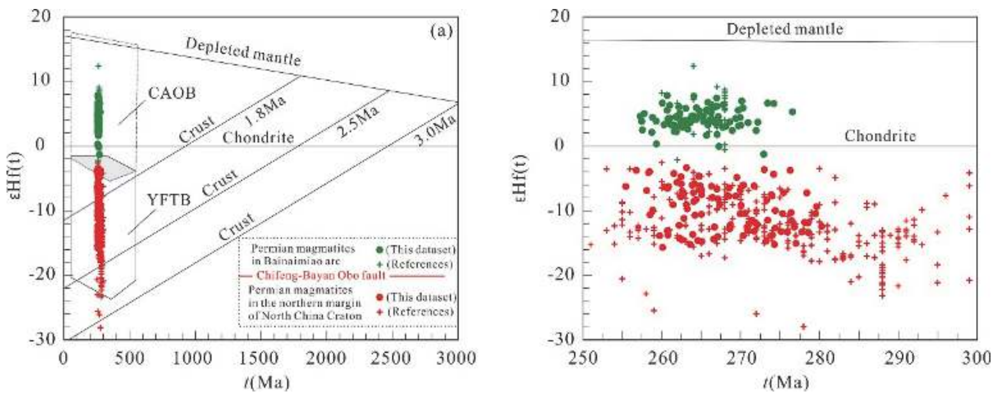

Fig. 2 The $\varepsilon_{Hf}(t)$-t diagram *of* Permian magmatites in the study area (referred data points are from Zhang SH et al., 2009, 2016; Dong XJ et al., 2016; Zhu XF et al., 2018; Zhou H et al., 2019)

exploration of the petrogenesis and tectonic-magmatic evolution process.

Two regional geological survey projects on a scale of 1 : 50 000 cover the junction between the northern margin of the North China Craton and Bainaimiao arc. One involves four map sheets in Inner Mongolia including the Beiliutumiao map sheet (K49E011021), Taigushengmiao map sheet (K49E011022), Xinminsumu map sheet (K49E012021) and Zhangmaowusu map sheet (K49E012022) (hereinafter referred to as the Regional Geological Survey Project of Four Map Sheets including the Beiliutumiao Map Sheet). The other covers two map sheets in Inner Mongolia including the Wulanbulage map sheet (K49E013008) and Baiyin Obo map sheet (K49E013009) (hereinafter referred to as the Regional Geological Survey Project of Two Map Sheets including the Wulanbulage Map Sheet). The Chifeng–Bayan Obo fault passes through the middle part of the study area and Permian magmatites are pervasively exposed in the study area. Given all these aspects, the dataset of the chronology, geochemistry and zircon Hf isotopes of Permian magmatites on the southern and northern sides of the fault will provide important data support for for researchinto the material composition of the provenance and tectonic-magmatic evolution processes of Permian magmatites in the study area.

The brief metadata table of the Dataset (Wang WL et al., 2020) is shown in Table 1.

2 Methods for Data Acquisition and Processing

2.1 Sampling

The Permian magmatite samples were taken from two projects. One project is localized in the southern part of Zhurihe and named the ‘Regional Geological Survey Project of Four Map Sheets including the Beiliutumiao Map Sheet’ (work area: 113°00′–113°30′E, 42°00′–42°20′N). The other is localized in the northwestern part of the Damao Banner and named the ‘Regional Geological Survey Project of Two Map Sheets including the Wulanbulage Map Sheet’ (work area: 109°45′–110°15′E, 41°50′–42°00′N). The work content of the first project covers zircon U–Pb dating, zircon Hf isotopic analysis, and whole-rock geochemical analysis of Permian intrusions. To this end, the samples of quartz diorite, granodiorite and

Table 1 Metadata Table of Database (Dataset)

Items	Description
Database (dataset) name	Dataset of Chronology, Geochemistry and Zircon Hf Isotopes of Permian Magmatites in the Middle Section of the Northern Margin of North China Craton
Database (dataset) authors	Wang Wenlong, Tianjin Center, China Geological Survey Liu Yang, Tianjin Center, China Geological Survey Zhao Ligang, Tianjin Center, China Geological Survey Teng Fei, Tianjin Center, China Geological Survey Yang Zeli, Tianjin Center, China Geological Survey
Data acquisition time	2016–2019
Geographic area	Geographical coordinates of the Regional Geological Survey Project of Four Map Sheets including the Beiliutumiao Map Sheet: 113°00′–113°30′E, 42°00′–42°20′N; Geographical coordinates of the Regional Geological Survey Project of Two Map Sheets including the Wulanbulage Map Sheet: 109°45′–110°15′E, 41°50′–42°00′N
Data format	*.xls
Data size	948 KB
Data service system URL	http://dcc.cgs.gov.cn
Fund project	Geological survey projects initiated by China Geological Survey (DD20160041, DD20190038)
Language	Chinese
Database (dataset) composition	The Dataset consists of three Excel files, namely *Zircon U–Pb dating data.xls, Zircon Hf isotope data.xls*, and *Whole-rock geochemistry data.xls*. Each of these files contains of two separate worksheets named *Data of Regional Geological Survey Project of Four Map Sheets including the Beiliutumiao Map Sheet* and *Data of Regional Geological Survey Project of Two Map Sheets including the Wulanbulage Map Sheet*. *Zircon U–-Pb dating data.xls* is comprised of the data on zircon U–Pb dating of 16 samples (401 testing points in total). *Zircon Hf isotope data.xls* is comprised of the data on zircon Hf isotopes of 12 samples (191 testing points in total). *Whole-rock geochemistry data.xls* is comprised of whole-rock geochemical data of 104 test samples

monzogranite were collected, including 10 samples for zircon U–Pb dating, nine samples for zircon isotopic analysis, and 77 samples for whole-rock geochemical analysis. The second project covers the work of zircon U–Pb dating, zircon Hf isotopic analysis, and whole-rock geochemical analysis of Permian intrusions and volcanics. The intrusions mainly include granodiorite and monzogranite. The volcanics mainly consist of andesitic, dacitic, rhyolitic pyroclastic rocks, and a small number of volcanic lavas. The samples collected in the second project include six for zircon U–Pb dating, three for zircon isotopic analysis, and 27 for whole-rock geochemical analysis (see the Dataset for detailed information of the samples, including numbers, rock types and sampling locations).

2.2 Testing Methods

2.2.1 Zircon U–Pb Dating and Hf Isotope Analysis

Fresh samples for zircon dating were taken in the field. The zircons in the samples were separated at the Hebei Institute of Regional Geological and Mineral Resource Survey. The samples were successively processed by a simple wash with water, high-intensity magnetic electromagnetic separation and elutriation of fines with alcohol. Finally, the zircons with large grain size and complete shape were sorted under a microscope. Testing targets of zircons were prepared at Beijing GeoAnalysis Co., Ltd. Cathodoluminescence imaging was conducted using a JSM_6510 series scanning electron microscope. The zircon U–Pb dating and the in-situ Hf isotopic analyses were completed at the Tianjin Center, China Geological Survey using laser ablation multiple collector inductively coupled plasma mass spectrometry (LA-MC-ICP-MS). A NEW WAVE 193-FXArF excimer laser was connected to a Neptune MC-ICPMS manufactured by Thermo Fisher Scientific Inc. The ablated material was transported by a He carrier gas. For zircon U–Pb dating, the laser beam spot adopted was 35 μm in diameter and the ablation duration was 30 s. GJ-1 zircon served as standards for fractionation correction of U, Th and Pb isotopes in the zircons. NIST610 glass was used as an external standard to calculate the content of U, Th and Pb in the zircons. During the dating, two points of a GJ-1 standard sample were tested at an interval of every eight testing points of the zircon samples. The weighted average $^{206}Pb/^{238}U$ age of GJ-1 was 600 Ma.

The in-situ micro-area Hf isotope analysis of the zircons was conducted using the laser and mass-spectrometer used in U–Pb dating. The laser beam spot for ablation used for the analysis was 50 μm in diameter and the ablation lasted for 30 s. GJ-1 zircon served as an external standard to calculate the ratio between Hf isotopes. During the analysis, two points of a GJ-1 standard samples were tested at an interval of every eight testing points of the zircon samples. The $^{176}Hf/^{177}Hf$ and $^{176}Lu/^{177}Hf$ ratios of GJ-1 were tested to be 0.282019 ± 0.000024 (2σ, n=57) and 0.00030 (n=57), respectively. Detailed instrument configuration and the experimental processes are described in Li HK et al. (2010) and Geng JZ et al. (2011). The data concerning U–Pb dating and Hf isotopes were processed using the ICPMSDataCal program (Liu YS et al., 2010).

2.2.2 Whole-rock Geochemistry

Fresh rock samples for whole-rock geochemical analysis were taken in the field. They were successively cleaned with water, dried in the air, mechanically crushed into 200 mushes and sent to at the Tianjin Center, China Geological Survey for testing of major and trace elements in the samples. The major elements were determined by the X-ray fluorescence (XRF) spectrometry with the fusion method. FeO was determined as follows. Firstly, the rock samples were dissolved using hydrofluoric and sulfuric acid. Then FeO was measured by titration—a type of volumetric analysis—using potassium bichromate, with a precision value lower than 2%. The trace elements were tested by ICP–MS, with a precision value lower than 5%. The samples were tested in accord with GB/T 14506-2010 in an environment where the temperature was 20 ℃ and the relative humidity was 30%, with GBW07104, GBW07105, GBW07111, and GBW07122 as standard samples.

3 Description of Data Samples

The Dataset consists of three Excel files, which are '*Zircon U–Pb dating data.xls*', '*Zircon Hf isotope data.xls*' and '*Whole-rock geochemistry data.xls*'. Each file contains two separate worksheets: '*Data of Regional Geological Survey Project of Four Map Sheets including the Beiliutumiao Map Sheet*' and '*Data of Regional Geological Survey Project of Two Map Sheets including the Wulanbulage Map Sheet*'.

The file '*Zircon U–Pb dating data.xls*' consists of information on zircon U–Pb dating of 16 samples taken from the study area. Each worksheet of this file is comprised of sample data such as sample no., sampling location, rock type, analysis point no., Th/U, isotope ratio, age and error. The file '*Zircon Hf isotope data.xls*' consists of data from zircon Hf isotope testing of 12 samples taken from the study area. Each worksheet of this file comprises the sample data such as sample no., analysis point no., zircon age, isotope ratio, $\varepsilon_{Hf}(t)$ and model age. The file '*Whole-rock geochemistry data.xls*' consists of the analytical results of major and trace elements in 104 samples taken from the study area. Each worksheet of this file comprises the sample data such as sample no., rock type and results from whole-rock geochemical analysis (See the Dataset for details).

4 Data Quality Control and Assessment

The zircon U–Pb dating, Hf isotope testing and whole-rock geochemical analyses were all conducted at the Tianjin Center, China Geological Survey by the methods and processes strictly consistent with applicable international standards (Ren JP et al., 2019; Wang SQ et al., 2019). Since the Permian magmatites to be tested have not experienced obvious metamorphism and metasomatism, the rock samples are considered 'fresh'. The zircons in the samples for U–Pb dating are intact in crystal form, with zonal structures developing. However, fissures exist in some zircons owing to the effect of late tectonic stress and testing points should be kept away from the zircon fissures (Li C et al., 2018). The LA-ICP-MS zircon U–Pb dating was conducted using the same methods as those adopted by Hou KJ et al. (2009) and the Hf isotope analysis was conducted using similar methods as those adopted by Hou KJ et al., (2007). The results obtained for zircon ages and Hf isotope analyses are comparable with those achieved by other researchers (Wang WQ et al., 2013; Dong XJ et al., 2016; Zhu XF et al., 2018; Zhou H et al., 2019).

5 Conclusion

The Dataset consists of three Excel data files named '*Zircon U–Pb dating data.xls*', '*Zircon Hf isotope data.xls*', and '*Whole-rock geochemistry data.xls*', which comprise data on zircon U–Pb dating of 16 samples, the data on zircon Hf isotopes of 12 samples and whole-rock geochemical data of 104 test samples, respectively. The Dataset will provide critical basic data for research on the material composition of the provenance and tectonic-magmatic evolution processes of Permian magmatites in the study area.

Acknowledgements: We would like to extend our sincere appreciation to two anonymous reviewers for their valuable suggestions on the modifications to this paper.

References

Bureau of Geology and Mineral Resources of Nei Mongol Autonomous Region. 1991. Regional Geology of Nei Mongol (Inner Mongolia) Autonomous Region[M]. Beijing: Geological Publishing House, 1−725(in Chinese with English abstract).

Champion DC, Bultitude RJ. 2013. The geochemical ang Sr-Nd isotopic characteristics of Paleozoic fractionated S-types granites of north Queensland: Implications for S-type granite petrogenesis[J]. Lithos, 162−163: 37−56.

Chen Y, Zhang ZC, Qian XQ, Li JF, Ji ZJ, Wu TR. 2020. Early to mid-Paleozoic magmatic and sedimentary records in the Bainaimiao Arc: An advancing subduction-induced terrane accretion along the northern margin of the North China Craton[J]. Gondwana Research, 79: 263−282.

Clemens JD, Stevens G, Farina F. 2011. The enigmatic sources of I-type granites: The peritectic connexion[J]. Lithos, 126: 174−181.

Dong Xiaojie, Wang Wanqiong, Sha Qian, Zhang Jinfeng. 2016. Suzy volcanic rocks in the northern margin of the North China Craton and its formation mechanism[J]. Acta Petrologica Sinica, 32(9): 2765−2779 (in Chinese with English abstract).

Geng Jianzhen, Li Huaikun, Zhang Jian, Zhou Hongying, Li Huimin. 2011. Zircon Hf isotopes analysis by means of LA-MC-ICP-MS[J]. Geological Bulletin of China, 30: 1508−1513 (in Chinese with English abstract).

Han BF, He GQ, Wang XC, Guo ZJ. 2011. Late Carboniferous collision between the Tarim and Kazakhstan eYili terranes in the western segment of the South Tian Shan Orogen, Central Asia, and implications for the Northern Xinjiang, western China[J]. Earth-Science Reviews, 109: 74−93.

Hou Kejun, Li Yanhe, Zou Tianren, Qu Xiaoming, Shi Yuruo, Xie Guiqing. 2007. Laser ablation-MC-ICP-MS technique for Hf isotope microanalysis of zircon and its geological applications[J]. Acta Petrological Sinica, 23(10): 2595−2604 (in Chinese with English abstract).

Hou Kejun, Li Yanhe, Tian Yourong. 2009. In situ U-Pb zircon dating using laser ablation-multi ion counting-ICP-MS[J]. Mineral Deposits, 28(4): 481−492 (in Chinese with English abstract).

Jahn BM, Wu FY, Chen B. 2000. Massive granitoid generation in Central Asia: Nd isotope evidence and implication for continental growth in the Phanerozoic[J]. Episodes, 23: 82−92.

Li Chong, Ren Liudong. 2018. The dataset of zircon geochronological & geochemical testing ofQingyuan Complex in Northern Liaoning province[J]. Geology in China, 45(S1): 140−150.

Li Huaikun, Zhu Shixing, Xiang Zhenqun, Su Wenbo, Lu Songnian, Zhou Hongying, Gen Jianzhen, Li Sheng, Yang Fengjie. 2010. Zircon U-Pb dating on tuffbed from Gaoyuzhuang Formation in Yanqing, Beijing: Further constraints on the new subdivision of the Mesoproterozoic stratigraphy in the northern North China Craton[J]. Acta Petrologica Sinica, 26(7): 2131−2140 (in Chinese with English abstract).

Liu YS, Gao S, Hu ZC, Gao CG, Zong KQ, Wang DB. 2010. Continental and oceanic crust recycling-induced melt-peridotite interactions in the Trans-North China Orogen: U-Pb dating, Hf isotopes and trace elements in zircons from mantle xenoliths[J]. Journal of Petrology, 51: 537−571.

Luo Hongling, Wu Tairan, Zhao Lei. 2009. Zircon SHRIMP U-Pb dating of Wuliangsitai Atype granite on the northern margin of the North China Plate and tectonic significance[J]. Acta Petrologica Sinica, 25(3): 515−526 (in Chinese with English abstract).

Luo Zhaohua, Huang Zhongmin, Ke Shan. 2007. Basic problems of granitic rocks[J]. Geological Review, 53(S1): 180−226 (in Chinese).

Ren Junping, Wang Jie, Gu Alei, Zuo Libo, Sun Hongwei, Xu Kangkang, Wu Xingyuan. 2019. Zircon U-Pb geochronology and Lu-Hf isotopic composition of syenogranite, northeastern Zambia[J]. Geological Survey and Research, 42(3): 161−165 (in Chinese with English abstract).

Sengör AMC, Natal'in BA, Burtman VS. 1993. Evolution of Altaid tectonic collageand Paleozoic crustal growth in Eurasia[J]. Nature, 364: 299−307.

Wang Shijie, Xu Zhongyuan, Dong Xiaojie, Wang Wanqiong, Li Pengchuan. 2018. Geochemical characteristicsand zircon U-Pb age of the granodiorite-norite gabbro in the northern margin of the North China Block and their formation mechanism[J]. Earth Science, 43(9): 3267−3284 (in Chinese with English abstract).

Wang Shuqing, Hu Xiaojia, Zhao Hualei. 2019. Geochronology of Late Carboniferous alkaline granite from Honger area, Sunidzuoqi, Inner Mongolia[J]. Geological Survey and Research, 42(2): 81−85 (in Chinese with English abstract).

Wang Wanqiong, Xu Zhongyuan, Liu Zhenhong, Zhao Qingying, Jiang Xiaojun. 2013. Early-Middle Permian tectonic evolution of the central-northern margin of the North China Craton: constraints from zircon u-pb ages and geochemistry of the granitoids[J]. Acta Petrologica Sinica, 29(9): 2987−3003 (in Chinese with English abstract).

Wang Wenlong, Liu Yang, Zhao Ligang, Teng Fei, Yang Zeli. 2020. Dataset of Chronology, Geochemistry and Zircon Hf Isotopes of Permian Magmatites in the Middle Section of the Northern Margin of North China Craton[DB/OL]. Geoscientific Data & Discovery Publishing System. (2020-06-30). DOI: 10.35080/data.A.2020.P4.

Wang Xiaolei. 2017. Some new research progresses and main scientific problems of granitic rocks[J]. Acta Petrologica Sinica, 33(5): 1445−1458 (in Chinese with English abstract).

Windley BF, Alexeiev D, Xiao W, Kröner A, Badarch G. 2007. Tectonic models for accretion of the Central Asian Orogenic Belt[J]. Journal of the Geological Society of London, 164: 31−47.

Xiao WJ, Windley BF, Hao J, Zhai MG. 2003. Accretion leading to collision and the Permian Solonker suture, Inner Mongolia, China: termination of the central Asian orogenic belt[J]. Tectonics, 22: 1069.

Xiao WJ, Windley BF, Sun S, Li J, Huang B, Han C, Yuan C, Sun M, Chen H. 2015. A tale of amalgamation of three permo-triassic collage systems in central Asia: oroclines, sutures, and terminal accretion[J]. Annual Review of Earth and Planetary Sciences, 43: 477−507.

Zhang SH, Zhao Y. 2017. Cogenetic origin of mafic microgranular enclaves in calc-alkaline granitoids: The Permian plutons in the northern North China Block[J]. Geosphere, 13: 482−517.

Zhang SH, Zhao Y, Ye H, Liu JM, Hu CZ. 2014. Origin and evolution of the Bainaimiao arc belt: implications for crustal growth in the southern Central Asian Orogenic Belt[J]. Geological Society of America Bulletin, 126: 1275−1300.

Zhang SH, Zhao Y, Ye H, Liu JM, Hu ZC. 2016. Different sources involved in generation of continental arc volcanism: The Carboniferous-Permian volcanic rocks in the northern margin of the North China block[J]. Lithos, 240−243: 382−401.

Zhang SH, Zhao Y, Kröner A, Liu XM, Lie WX, Chen FK. 2009. Early Permian Plutons from the Northern North China Block: Constraints on Continental Arc Evolution and Convergent Margin Magmatism Relatedtothe Central Asian Orogenic Belt[J]. International Journal of Earth Sciences, 98(6): 1441−1467.

Zhao P, Chen Y, Xu B, Faure M, Shi G, Choulet F. 2013. Did the Paleo-Asian Ocean between North China Block and Mongolia Block exist during the late Paleozoic? First paleomagnetic evidence from central-eastern Inner Mongolia, China[J]. Journal of Geophysical Research, Solid Earth, 118: 1873−1894.

Zhou H, Zhao GC, Han YG, Wang B. 2018. Geochemistry and zircon U-Pb-Hf isotopes of Paleozoic intrusive rocks in the Damao area in Inner Mongolia, northern China: Implications for the tectonic evolution of the Bainaimiao arc[J]. Lithos, 314−315: 119−139.

Zhou H, Zhao GC, Li JH, Han YG, Yao JL, Wang B. 2019. Magmatic evidence for middle-late Permian tectonic evolution on the northern margin of the North China Craton[J]. Lithos, 336−337: 125−142.

Zhou JB, Wilde SA, Zhao GC, Han J. 2018. Nature and assembly of microcontinental blocks within the Paleo-Asian Ocean[J]. Earth Science Reviews, 186: 76−93.

Zhu Xuefeng, Chen Yanjing, Wang Pin, Zhang Cheng, Cai Yunlong, Deng Ke, Xu Qiangwei, Li Kaiyue. 2018. Zircon U-Pb age, geochemistry and Hf isotopes of the causative porphyry from the Bilihe porphyry gold deposit, Inner Mongolia[J]. Earth Science Frontiers, 25(5): 120−134 (in Chinese with English abstract).